Available online at www.sciencedirect.com
ScienceDirect
Vibrational Spectroscopy 43 (2007) 313–318
VIBRATIONAL SPECTROSCOPY
www.elsevier.com/locate/vibspec

Structural properties of silver nanoclusters–phosphate glass composites

L. Baia [a,b,*], D. Muresan [a], M. Baia [a,b], J. Popp [b], S. Simon [a]

[a] Faculty of Physics, Babes-Bolyai University, M. Kogalniceanu 1, 400084 Cluj-Napoca, Romania
[b] Institute of Physical Chemistry, Friedrich-Schiller-University, Helmholtzweg 4, D-07743 Jena, Germany

Received 30 January 2006; received in revised form 17 March 2006; accepted 20 March 2006
Available online 3 May 2006

Abstract

The structure of the $xAg_2O(100-x)[50P_2O_5{\cdot}30CaO{\cdot}20Na_2O]$ glasses, with $x = 0$, 3 and 5 mol%, was investigated by means of Raman and infrared spectroscopy. The structural changes induced by the Ag_2O presence into the soda-calcium–phosphate matrix were evidenced and discussed in terms of the network depolymerization process and distortion of the PO_4 tetrahedra. The existence of silver nanoclusters inside the glass matrix, considered to be mainly responsible for the found structural behavior, was supposed by results obtained from the analysis of the UV–vis absorption spectra and further proved by transmission electron microscopy images.

Keywords: Raman; IR; UV–vis; TEM; Phosphate glasses; Silver nanoclusters; Composites

1. Introduction

In the last decades phosphate based glasses have been of interest for a variety of applications due to their several special properties such as large thermal expansion coefficients, low melting temperatures, solubility, etc. [1–5]. Because the glass chemical composition can be easily chosen to match the natural bone, these amorphous structures have a great potential for use as biomaterials [4]. Recently [4], a new type of phosphate glass for tissue engineering ($50P_2O_5{\cdot}30CaO{\cdot}20Na_2O$) has been obtained, good biocompatibility and low toxicity being expected. Phosphate glasses are composed of PO_4 tetrahedra that could be bound to one (Q^1 species), two (Q^2 species) and three (Q^3 species) other tetrahedra through the formation of P–O–P bonds at the tetrahedra corners [6–8]. The addition of definite amounts of metal ions, such as Ca^{2+} and Na^+, could produce significant changes of the phosphate glass structure from a three-dimensional random network to long or very short chains of PO_4 tetrahedra [4,9]. Generally, the introduction of Ag_2O into the bioactive glass composition is aimed to minimize the risk of microbial contamination by taking the advantage of the potential antimicrobial activity of the leaching Ag^+ ions [10]. The introduction of silver has recently became one of the preferred methods that confers microbial resiliency on biomedical materials and devices, since the incidence of biomaterial—centered infections is one of the main causes of revision surgery [11–14].

The understanding of the glasses structure on different length scales remains difficult mainly due to the lack of periodicity inherent to glasses. Only the suitable correlation of experimental data obtained from several investigations provided by different methods allows the finding of helpful structural information. The use of complementary techniques such as Raman, infrared (IR) and UV–vis spectroscopy has proven to be an efficient examination way of the glasses structure, in general [15–19], and of the phosphate glasses structure, in particular [1,2,8,20–22].

The aim of this study is to obtain valuable information concerning the structure of glasses with the general composition $xAg_2O(100-x)[50P_2O_5{\cdot}30CaO{\cdot}20Na_2O]$, with $x = 0$, 3 and 5 mol%, by means of Raman and IR spectroscopy. We are interested to get further insights into the glasses structure with the help of UV–vis spectroscopy and transmission electron microscopy (TEM) and to correlate these findings with those obtained from Raman and IR investigations.

2. Experimental

Glass samples belonging to $xAg_2O(100-x)[50P_2O_5{\cdot}30CaO{\cdot}20Na_2O]$, with $x = 0$, 3 and 5 mol% were prepared

* Corresponding author. Tel.: +40 264 405300; fax: +40 264 591906.
E-mail address: lucb@phys.ubbcluj.ro (L. Baia).

0924-2031/$ – see front matter
doi:10.1016/j.vibspec.2006.03.006

using as starting materials $NH_4H_2PO_4$, $CaCO_3$, $Na_2CO_3 \cdot 10H_2O$, and Ag_2O of reagent purity grade. The mixtures corresponding to the desired compositions were melted together at once in air, in sintered corundum crucibles, in an electric furnace Carbolite RF 1600 at 1200 °C and maintained for 15 min at this temperature. The melts were quickly cooled at room temperature by pouring and pressing between two stainless steel plates.

Confocal Raman measurements were performed on a Dilor Labram system equipped with a 100×0.90 microscope objective, a 1800 lines/mm grating and an external laser with an emission wavelength of 514.5 nm. In the recording of the micro-Raman spectra a power of 100 mW incident on the sample has been employed. Samples were mounted on a x, y motorized stage, and the z-displacement was controlled by a piezo-transducer on the objective. For all measurements the confocal pinhole diameter was 200 μm and the slit width was 40 μm. The confocal depth of focus in air, estimated by z-scanning of a silicon wafer, was measured to be ~2 μm. The spectral resolution was of about 2 cm^{-1}. The acquisition time required for the recording of each spectrum was of 120 s.

For IR measurements the glasses were powdered and mixed with KBr in order to obtain thin pellets. The IR spectra were recorded with a Bruker Equinox 55 spectrometer. The spectral resolution in this case was 2 cm^{-1}.

UV–vis absorption measurements on the as-prepared samples were performed with a Cary 5000 UV–vis–NIR spectrometer.

A JEOL JEM 1010 transmission electron microscope (TEM) was used to evidence the existence of the silver nanoparticles, which were formed into the glass matrix. Prior performing TEM measurements the glass samples were dissolved in HF and sonicated. The resulted suspensions were well washed with distilled water and deposited on a holey carbon film supported by a copper grid. The nanoparticle sizes were determined by using the Image Processing and Analysing software.

3. Results and discussion

The Raman and IR spectra of the investigated samples are displayed in Figs. 1 and 2 and the observed bands together with their assignment are listed in Table 1. By looking at the Raman spectra a few structural changes can be observed as a result of the Ag_2O presence into the phosphate glass matrix. Thus, especially for the glass with the smallest Ag_2O content ($x = 3$) one can remark a slight increase in intensity of the bands and shoulders at 340, 755 and 1045 cm^{-1} and attributed to the O–P–O bending, P–O–P stretching vibrations in various PO_4 tetrahedra and asymmetric stretching vibrations of $(PO_3)^{2-}$ (Q^1 species), respectively [8,9,23–25], in comparison with those that occur in the spectra of the glass matrix and the sample with higher Ag_2O content ($x = 5$). While the increase in intensity of the 340 cm^{-1} band could be associated with the presence of distorted PO_4 tetrahedra, the enhancement of the 1045 cm^{-1} band shows the increase of the number of nonbridging oxygen. Concerning the shoulder at around 755 cm^{-1} it was shown that the asymmetry on the high energy

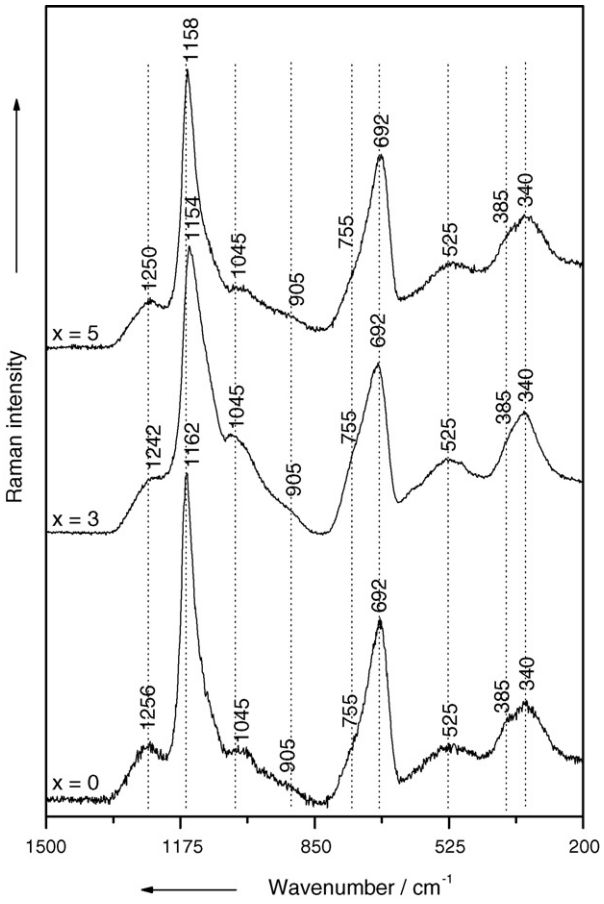

Fig. 1. Raman spectra of the $xAg_2O(100 - x)[50P_2O_5 \cdot 30CaO \cdot 20Na_2O]$ glasses.

side of the band around 692 cm^{-1}, which is assigned to the P–O–P stretching vibrations of the long-chain species, is caused by the increase of the number of very short chain phosphate units or ring structures [1]. A careful inspection of the Raman spectra (Fig. 1) reveals the existence of a similar asymmetry of the band with the maximum at 692 cm^{-1}, especially in the spectrum recorded on the glass with the smallest Ag_2O content ($x = 3$). Thus, the distinguished appearance of the shoulder around 755 cm^{-1} corroborated with the above-mentioned increased number of Q^1 species found for this glass indicates the occurrence of a more pronounced fragmentation of the connected phosphate network. In order to ensure about the accuracy of the unusuall structural changes revealed by Raman spectra that take place as the Ag_2O content increases several measurements on different samples have been performed by using a confocal set-up. The similar spectral caracteristics, i.e. band position and relative intensities, observed in the spectra quarantee the samples homogeneous structure and the correctness of the obtained results.

The particular structural behaviour observed for the sample with 3 mol% Ag_2O is further mirrored by Raman features recorded at around 1162 and 1256 cm^{-1}, for $x = 0$, and attributed to the $(PO_2)^-$ (Q^2 species) stretching vibrations [8]. These bands are shifted to smaller wavenumber values as the Ag_2O content becomes higher. Surprisingly, the wavenumber

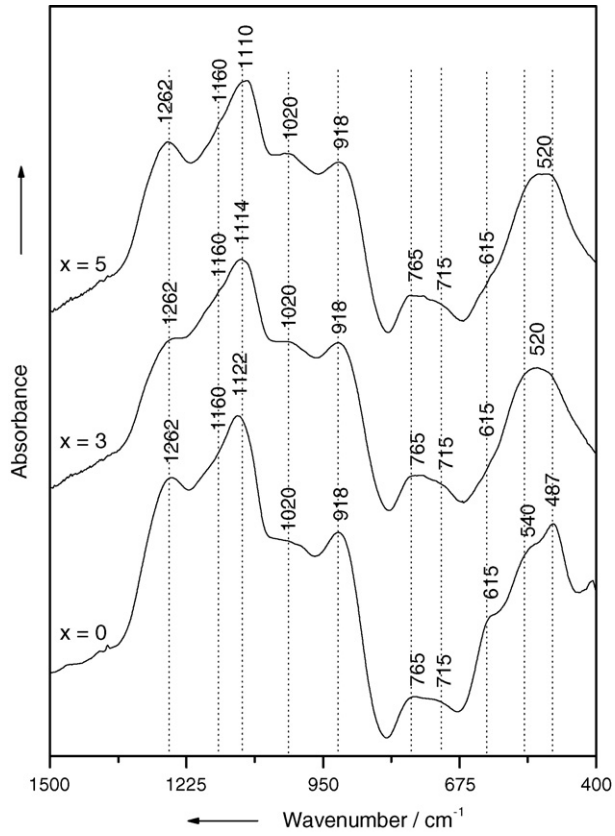

Fig. 2. IR spectra of the $xAg_2O(100-x)[50P_2O_5{\cdot}30CaO{\cdot}20Na_2O]$ glasses.

values where these bands appear are located between those of the corresponding bands recorded for the glass matrix and the sample with 5 mol% Ag_2O. Taking into account that vibrations of the $(PO_2)^-$ and $(P_2O_7)^{4-}$ (Q^2 and $2Q^1$ species) give Raman bands in the 1130–1065 cm^{-1} spectral range [8] and that the Raman band with the maximum located at 1162 cm^{-1} broadens for $x = 3$ it becomes plausible that at this concentration fractions of the Q^2 species form $2Q^1$ species. On the other hand, these structural changes cause a distortion of the PO_4 tetrahedra as it was before evidenced in the Raman spectra by the shift and broadening of the band located around 1256 cm^{-1}, for $x = 0$. Taking into account these spectral modifications we can conclude that the silver oxide presence into the phosphate glass matrix leads both to the appearance of a depolymerization process of the phosphate network as well as to the distortion of the PO_4 tetrahedra, especially when the Ag_2O amount is small ($x = 3$). However, it is remarkable that no significant spectral changes arise for the band located around 905 cm^{-1} and attributed to the $(PO_4)^{3-}$ (Q^0 species) symmetric stretching vibrations. This result shows that a considerable part of the phosphate network still remains linked.

By looking at the IR spectra (Fig. 2) one can see the increase in intensity of the bands around 540 and 1020 cm^{-1} assigned to P–O–P bending and $(PO_3)^{2-}$ (Q^1 species) stretching vibrations, respectively, as the Ag_2O content increases. One can also remark a shift to smaller wavenumber values of the band at 1122 cm^{-1} that was attributed to $(PO_3)^{2-}$ (Q^1 species) stretching vibrations [8]. A very small raise in intensity of the absorption signal recorded between 1155 and 1170 cm^{-1} and due to the $(PO_2)^-$ (Q^2 species) vibrations can be also observed, especially for $x = 3$. At the same concentration appears a slight decrease of the 1262 cm^{-1} band assigned to P=O vibrations [8,26]. All above-mentioned spectral changes confirm and further complete the results obtained from Raman spectra analysis, evidencing both the distortion of the PO_4 units as a result of the Ag_2O presence as well as the alteration of the P=O bond for the smallest silver content. The evolution of the

Table 1
Raman and IR band assignments for $xAg_2O(100-x)[50P_2O_5{\cdot}30CaO{\cdot}20Na_2O]$ glasses

Wavenumber (cm^{-1})						Assignment[a]
$x = 0$ mol%		$x = 3$ mol%		$x = 5$ mol%		
Raman	IR	Raman	IR	Raman	IR	
340		340		340		δ(O–P–O)
385		385		385		δ(O–P–O)
	487					δ(P–O–P)
525	540	525	520	525	520	δ(P–O–P)
	615		615		615	δ(P–O–P)
692	715	692	715	692	715	ν_s(P–O–P)
755	765	755	765	755	765	ν_s(P–O–P)
905	918	905	918	905	918	$\nu_s(PO_4)^{3-}$
	1020		1020		1020	$\nu_s(PO_3)^{2-}$
1045		1045		1045		$\nu_{as}(PO_3)^{2-}$
	1122		1114		1110	$\nu_{as}(PO_3)^{2-}$
1130–1065		1130–1065		1130–1065		$\nu_s(PO_2)^-$ and $\nu_s(P_2O_7)^{4-}$
1162	1158	1158	1158	1157	1158	$\nu_s(PO_2)^-$
1256	1262	1242	1262	1250	1262	$\nu_{as}(PO_2)^-$

Abbreviations: δ, deformation; ν, stretching; s, symmetric; as, asymmetric.
[a] Refs. [8,9,23–26].

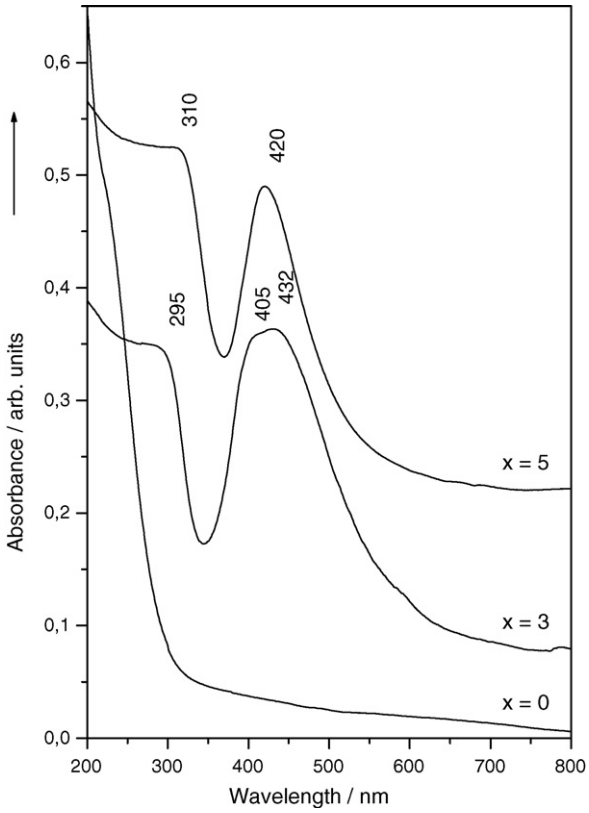

Fig. 3. UV–vis absorption spectra of the xAg$_2$O$(100-x)$[50P$_2$O$_5$·30CaO·20Na$_2$O] glasses.

IR bands and shoulders recorded around 765 and 715 cm^{-1} for $x = 0$, as the Ag$_2$O content increases, does not reveal so clear as in the Raman spectra the gradual transformation of the long chains phosphate units or ring structures into linked phosphate units of shorter lengths.

In order to get further insides into the structure of the investigated glasses UV–vis absorption spectra were recorded and are presented in Fig. 3. Absorption bands were evidenced only for the glass samples containing silver. It was reported [27] that besides the pronounced silver plasmon resonances that appear between 400 and 500 nm, the electronic transitions involving the Ag^+ ion give rise to absorption bands located between 200 and 230 nm, whereas the electronic transitions of metallic Ag^0 appear in the 250–330 nm spectral range. By looking at the spectra shown in Fig. 3 one can see distinct absorption signals due to Ag^0 and plasmon resonances. The signature of the Ag^+ ion cannot be easily observed because of the electronic absorption signal given by the glass matrix that appears in the same spectral region. The close analysis of the spectra further reveals that for the sample with the highest silver oxide content ($x = 5$) the intensity of the band given by Ag^0 is higher than that due to the plasmon resonance. The convolution of the absorption signals given by the glass matrix and Ag^0 could explain the shift to longer wavelengths of the absorption band located around 300 nm for the sample with 5 mol% Ag$_2$O. In the spectrum of the sample with 3 mol% Ag$_2$O a broad plasmon resonance absorption band arises as a result of the convolution of the signals located around 405 and 432 nm, while in the spectrum of the sample with 5 mol% Ag$_2$O a singular absorption band appears at around 420 nm.

Theoretical and experimental studies of the optical properties of silver particles embedded in a glass matrix [15,28,29] have shown that the appearance of a band at around 400 nm in the electronic absorption spectrum is associated with the existence of very small, metallic spherical silver particles inside the glass matrix. It was also stated [8] that if the particles were not spherical (or equiaxial), the electronic absorption band would be at longer wavelengths and would gradually shift to shorter wavelengths as the particles became more spherical. On the other hand, it was theoretically shown [8,30] that above a certain particle size (≈10 nm), the absorption band begins to shift to longer wavelengths because additional magnetic-dipole terms appear for larger radii particles. It can be thus concluded that two factors, whose influence can be easier exploited with the help of standard investigation techniques, mainly contribute to the shift of the plasmon resonance absorption band to higher wavelength, the particles shape and size. Nevertheless, the optical properties of the composite materials sensitively depend on many other parameters such as density and spatial distribution of the nanoparticles or the surrounding environment of the host medium. Keeping in mind the above-mentioned assertions we are justified assuming that the appearance of the absorption signal at around 405 nm in the spectrum of the sample with 3 mol% Ag$_2$O is mainly due to the existence of almost spherical silver nanoparticles having small dimension within the phosphate glass matrix, while the absorption maximum at 432 nm is caused by nonspherical silver particles or/and particles with higher sizes. Similarly, the electronic absorption band at 420 nm recorded on the sample with 5 mol% Ag$_2$O is most probably due to the presence of nonspherical particles or/and particles with higher sizes compared to those that give rise to the band at 405 nm, but smaller than those which are assumed to give the band at 432 nm. The appearance of less spherical nanoparticles as silver particles become higher was also previously observed [27].

TEM pictures of these two composite materials are shown in Fig. 4. These images clarify, complete and confirm the majority of the above considerations. Thus, for the samples containing 3 mol% Ag$_2$O (Fig. 4(a)) one can observe small nanoparticles having dimensions around 10 nm (see the inset) as well as nonspherical particles, whose length sizes are between 40 and 100 nm. For the samples with the higher silver content (Fig. 4(b)) one can see spherical and nonspherical particles with dimensions between 20 and 40 nm. The analysis of the plasmon resonance bands intensity from the UV–vis absorption spectrum of the sample with 3 mol% Ag$_2$O permits us to assume that most of the silver nanoclusters inside this sample have sizes in the range 40–100 nm. Thus, it is important to note the existence of particles with small dimensions for the sample with 5 mol% Ag$_2$O in comparison with the main part of the particles found for the sample with smaller silver content. These findings corroborated with the results obtained from Raman and IR analysis provide other relevant conclusion. The presence of nanoparticles with sizes between 40 and 100 nm,

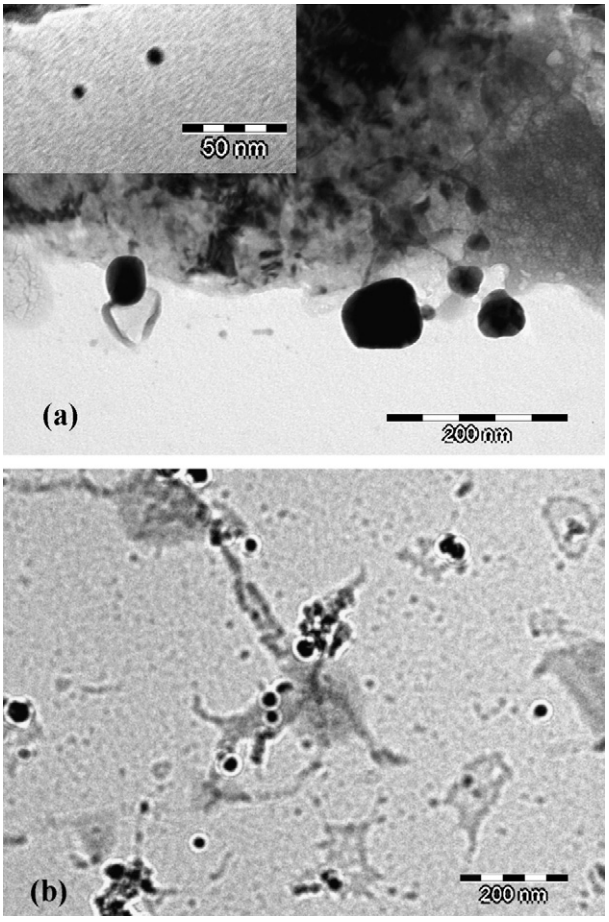

Fig. 4. TEM images of the $xAg_2O(100-x)[50P_2O_5{\cdot}30CaO{\cdot}20Na_2O]$ glasses: (a) $x = 3$ and (b) $x = 5$. The inset represents another image recorded for the sample with $x = 3$ at an enlarged scale.

which are considerable higher than those found for the glass with 5 mol% Ag_2O (between 20 and 40 nm), could explain the more pronounced depolymerization process occurred in the sample with the smallest Ag_2O content ($x = 3$) as revealed from Raman and IR spectra, due to the much consistent distortions induced by the nanoparticles of high dimensions to the phosphorus structural units situated in their close vicinity.

The above findings related to the morphological and structural particularities of the newly prepared silver nanoclusters–phosphate glass composites give confidence that such materials could be attractive for tissue engineering thanks to the silver presence that confer them antibacterial properties. Preliminary tests performed in our laboratories [31,32] have already proved the antibacterial effects of these composites.

4. Conclusion

Raman and IR spectroscopic investigations of the newly prepared $xAg_2O(100-x)$ $[50P_2O_5{\cdot}30CaO{\cdot}20Na_2O]$ glass system, with $x = 0$, 3 and 5 mol%, revealed that the silver oxide presence into the phosphate glass matrix leads both to the appearance of a network depolymerization process as well as to the distortion of the PO_4 tetrahedra, especially for the sample with the smallest Ag_2O amount. The silver nanoparticles existence into the soda-calcium–phosphate matrix was assumed from the analysis of the UV–vis absorption spectra and further proved by TEM images. The present structural investigations could open up new and attractive perspectives of using such composites in tissue engineering thanks to the silver presence that can provide them antibacterial properties.

Acknowledgements

The authors would like to thank Prof. Dr. W. Kiefer (University of Würzburg) and Prof. Dr. C. Craciun (Babes-Bolyai University) for providing access to equipments of their laboratories. L.B., M.B., and J.P. acknowledge financial support from the Deutsche Forschungsgemeinschaft (SFB 436, C1).

References

[1] J.E. Pemberton, L. Latifzahed, J.P. Fletcher, S.H. Risbud, Chem. Mater. 3 (1991) 195.
[2] I. Belharouak, C. Parent, B. Tanguy, G. Le Flem, M. Couzi, J. Non. Cryst. Solids 244 (1999) 238.
[3] J.E. Garbarczyk, P. Machowski, M. Wasiucionek, L. Tykarski, R. Bacewicz, A. Aleksiejuk, Solid State Ionics 136/137 (2000) 1077.
[4] I. Ahmed, M. Lewis, I. Olsen, J.C. Knowles, Biomaterials 25 (2004) 491.
[5] E.T.Y. Lee, E.R.M. Taylor, Opt. Mater. 28 (2006) 200.
[6] U. Hoppe, J. Non-Cryst. Solids 195 (1996) 138.
[7] M. Nocuń, J. Non-Cryst. Solids 333 (2004) 90.
[8] G. Le Saoüt, P. Simon, Fayon F. F., A. Blink, Y. Vaills, J. Raman Spectrosc. 33 (2002) 740.
[9] M. Hafid, T. Jermoumi, N. Niegisch, M. Mennig, Mater. Res. Bull. 36 (2001) 2375.
[10] A.G. Avent, C.N. Carpenter, J.D. Smith, D.M. Healy, T. Gilchrist, J. Non-Cryst. Solids 328 (2003) 31.
[11] M. Kawashita, S. Tsuneyama, Miyaji F. F., T. Kokako, H. Kozuka, K. Yamamoto, Biomaterials 21 (2000) 393.
[12] M. Bellantone, H.D. Williams, L.L. Hench, Antimicrob. Agents Chemother. 46 (2002) 1940.
[13] T.N. Kim, Q.L. Feng, J.O. Kim, J. Wu, H. Wang, G.C. Chen, J. Mater. Sci. Mater. Med. 9 (1998) 129.
[14] T. Matsuura, Y. Abe, Y. Sato, K. Okamoto, M. Ueshige, Y. Akagawa, J. Dent. 25 (1997) 373.
[15] P. Chakraborty, J. Mater. Sci. 33 (1998) 2235.
[16] L. Baia, R. Stefan, W. Kiefer, J. Popp, S. Simon, J. Non-Cryst. Solids 303 (2002) 379.
[17] L. Baia, R. Stefan, J. Popp, S. Simon, W. Kiefer, J. Non-Cryst. Solids 324 (2003) 109.
[18] A. Radu, L. Baia, W. Kiefer, S. Simon, Vib. Spectrosc. 39 (2005) 127.
[19] L. Baia, M. Bolboaca, W. Kiefer, E.S. Yousef, C. Rüssel, F.W. Breitbarth, T.G. Mayerhöfer, J. Popp, Phys. Chem. Glasses 45 (2004) 178.
[20] L. Baia, D. Muresan, E. Burean, V. Simon, W. Kiefer, S. Simon, in: P.M. Fredericks, R.L. Frsot, L. Rintoul (Eds.), Proceedings of the XIXth International Conference on Raman Spectroscopy (ICORS), CSIRO Publishing, Australia, 2004, p. 502.
[21] R.K. Brow, D.R. Tallant, J.J. Hudgens, S.W. Artin, A.D. Irwin, J. Non-Cryst. Solids 177 (1994) 221.
[22] J.J. Hudgens, R.K. Brow, D.R. Tallant, S.W. Artin, J. Non-Cryst. Solids 223 (1998) 21.
[23] S.T. Reis, D.L.A. Faria, J.R. Martinelli, W.M. Pontuschka, D.E. Day, C.S.M. Partiti, J. Non-Cryst. Solids 304 (2002) 188.
[24] D. Ilieva, B. Jivov, G. Bogachev, C. Petkov, I. Penkov, Y. Dimitriev, J. Non-Cryst. Solids 283 (2001) 195.
[25] B.Y. Matic, L. Börgerson, Philos. Mag. B 77 (2) (1998) 357.
[26] C. Dayanand, G. Bhikshamaiah, V. Jaya Tyagaraju, M. Salagram, A.S.R. Krishna Murthy, J. Mater. Sci. 31 (1996) 1945.

[27] J. Lu, J.J. Bravo-Suárez, A. Takahashi, M. Haruta, S.T. Oyama, J. Catal. 232 (2005) 85.
[28] W. Otter, Z. Phys. 161 (1961) 163.
[29] S. Link, M.A. El-Sayed, Annu. Rev. Phys. Chem. 54 (2003) 331.
[30] G. Mie, Ann. Phys. 25 (1908) 377.
[31] D. Muresan, C. Popa, M. Dragan-Bularda, L. Baia, S. Simon, Book of Abstracts of the International Conference Biomaterials & Medical Devices, Bucharest, 2004, p. 53.
[32] D. Muresan, M. Dragan-Bularda, C. Popa, L. Baia, S. Simon, Rom. J. Phys. 51 (2006) 213.